Relativistic corrections to the binding energy of positronic alkali-metal atoms

Takuma Yamashita [*]
Nishina Center, RIKEN, Wako, 351-0198, Japan
and Department of Chemistry, Tohoku University, Sendai, Miyagi 980-8578, Japan

Yasushi Kino [†]
Department of Chemistry, Tohoku University, Sendai 980-8578, Japan

(Received 21 August 2019; published 17 December 2019)

We report a theoretical calculation of the relativistic corrections to the binding energy of positronic alkali-metal atoms. The ground state for the positronic alkali-metal atom is a loosely bound state with the structure of an alkali-metal ion surrounded by a positronium cloud. The correlation between the valence electron and positron in the field of a residual core ion is taken into account using a three-body model. Relativistic corrections to the binding energy for positronic alkali-metal atoms are evaluated based on the Breit-Pauli perturbation theory up to the second order of the fine structure constant. The relativistic corrections caused by the interaction between the valence electron and core ion was evaluated from the decomposed expectation values of the perturbation Hamiltonian. We found that the importance of relativistic corrections to the binding energy, namely the ratio of the net relativistic correction in the total binding energy, is remarkably enhanced in the loosely bound states of positronic alkali-metal atoms, where the charge of the valence electron is screened by the positron as positronium in the outermost region, while the electron is released from the positron near the nucleus. The results imply that positronic atoms with a dominant positronium can serve as an apt testing ground for relativistic quantum mechanics.

DOI: 10.1103/PhysRevA.100.062511

I. INTRODUCTION

Some neutral atoms can bind a positron by themselves and form a bound-state, positronic atom. The positronic atom is one of the most fundamental systems in atomic physics and can exhibit the exotic aspects of atomic and molecular systems [1–3]. The binding mechanism, bound-state structure, and interparticle correlations in positronic atoms having simple electronic structure of the atom have been subject to precise calculations [4–8]. Attractive correlations of the positron and electrons in a positronic atom involve challenges in conventional theoretical approaches [9,10] hence require rigorous treatments. Further, the prediction of various positronic atoms [11–13], their resonance states [14–26] and formation or detection schemes of the bound states [27–30] have also attracted both theoretical and experimental attention [12,13]. The formation of positronium (Ps; a bound state of a positron and an electron) is a unique but fundamental reaction in positron-atom interaction, and still shows discrepancies in cross sections between theoretical calculations and experiments [31–36].

The positronic alkali-metal atom, which is a bound state of a positron and an alkali-metal atom (A), is one of the best models for positronic atoms because the alkali-metal atom can be well approximated by a valence electron and a residual closed-shell positive ion core (A^+). Long-range interaction due to the polarization of the ion core and short-range interactions associated with distributions of the ion core electrons can be taken into account by introducing a model potential that can reproduce the energy levels of the alkali-metal atom. The positronic alkali-metal atom can be treated as a three-body system, for which precise calculations are available.

There are a number of calculations on positronic alkali-metal atoms [2,4–6,35,37–45], where the major binding mechanism for a positronic alkali-metal atom is Ps polarization by A^+. When a positron attaches to A, the valence electron transfers to the positron and forms Ps because the ionization energy of A is smaller than the binding energy of Ps (6.8 eV). The residual ion core polarizes the Ps and forms a loosely bound state of the positronic alkali-metal atom (APs^+) just below the $A^+ + Ps$ threshold energy. Bound states of a positronic lithium atom ($LiPs^+$) and positronic sodium atom ($NaPs^+$) have been predicted theoretically, and positronic potassium and heavier alkali-metal atoms have been considered devoid of any bound state [12,13]. Calculations of the shallow binding energy are somewhat scattered depending on the choice of the model potential. Indeed, some arbitrariness remains in the short-range part of the model potential [44,45].

In this work, we investigate the binding mechanism of APs^+ in terms of relativistic effects. Relativistic effects in atomic and/or molecular systems have recently received considerable attention, and various studies of the electronic characteristics of heavy atoms have been conducted. Relativistic atomic physics and quantum chemistry focus on spin-forbidden chemical reactions, the unique structures of compounds (see Refs. [46,47] and references therein), and the atomic energy levels of highly charged ions for precise

[*]takuma.yamashita@riken.jp
[†]y.k@tohoku.ac.jp

tests of fundamental physics or for fundamental databases in astrophysics. In these studies, sixth- and seventh-period elements have often been the subject of research: the chemistry of gold compounds with various oxidation states [48–53], gold clusters [54,55], gold and platinum catalysts [56], heaviest elements [57,58], and reactions via spin-forbidden states [59]. Calculation methods in relativistic atomic physics and quantum chemistry have evolved recently, and various successful methods have been reported [60–63]. The importance of precise calculations of the relativistic wave function has also been recognized in connection with a search for the electron dipole moment (EDM) (for a review, e.g., see Ref. [64] and the references therein).

Relativistic corrections to the binding energy of positronic alkali-metal atoms have been considered unimportant, however, owing to the small atomic numbers of Li and Na. Some exhaustive surveys of e^+/Ps-atom complexes for large atomic number systems were performed within a relativistic framework by the first-order perturbation theory based on Hartree-Fock approximation [65] and a relativistic linearized coupled-cluster single-double approximation [66,67]. On the other hand, the effect of the relativistic corrections on binding energy of the positronic alkali-metal atoms, loosely bound states, is still unclear so far. The binding energy (ε) of the positronic alkali-metal atoms may be written in a sum of nonrelativistic binding energy ($\varepsilon^{\rm nr}$) and relativistic corrections ($\delta\varepsilon$) as $\varepsilon = \varepsilon^{\rm nr} + \delta\varepsilon$. The loosely bound states of the positronic alkali-metal atoms have been known to have extremely small ε; however, it is still an open question if the ratio of $\delta\varepsilon/\varepsilon$ becomes small or large in compared with conventional atomic systems because the physical origins of ε and $\delta\varepsilon$ and their trends may differ each other. In fact, a rough estimation using a simple potential approximation for positronic alkali-metal atoms [68,69] implies relativistic effects might appear in loosely bound states as large ratio $\delta\varepsilon/\varepsilon$.

Here, we calculate relativistic corrections of positronic alkali-metal atoms up to α^2 order, where α denotes the fine structure constant. The boundary conditions for the fine structure of neutral alkali-metal atoms will provide subsidiary improvement to the inner arbitrariness of model potentials. Further, we updated the binding energy with highly precise calculations using a relativistic framework, and the relativistic effects in the ground state were evaluated based on the roles of the fragment expectation values of the relativistic perturbation Hamiltonian.

The remainder of this paper is organized as follows. Section II introduces the theoretical concepts and calculations. Section III presents the results and discussion. Finally, conclusions are provided in Sec. IV. Except where mentioned otherwise, atomic units (a.u.; $m_{\rm e} = \hbar = e = 1$) are used throughout the present paper. The distance is expressed in unit of the Bohr radius a_0.

II. THEORY

The model potential between the ion core and valence electron is written as

$$V_{\rm e}(r_{\rm e}) = V_{\rm st}(r_{\rm e}) + V_{\rm exch}^{(l_{\rm e})}(r_{\rm e}) + V_{\rm pol}(r_{\rm e}), \tag{1}$$

where $V_{\rm st}(r_{\rm e})$ is the static potential given by the standard Hartree potential [70,71], $V_{\rm exch}^{(l_{\rm e})}(r_{\rm e})$ is the local exchange potential, $V_{\rm pol}(r_{\rm e})$ is the polarization potential, and $l_{\rm e}$ is the angular momentum quantum number for the electron.

The exchange potential was originally derived by Furness and McCarthy [72] and was modified by Gianturco and Scialla [73] for low-energy scattering calculations:

$$V_{\rm exch}(r_{\rm e}) = \tfrac{1}{2}\{(-V_{\rm st}(r_{\rm e}) + C_{\rm TF}(\rho_{\rm e}(r_{\rm e}))^{2/3}) - \sqrt{(-V_{\rm st}(r_{\rm e}) + C_{\rm TF}(\rho_{\rm e}(r_{\rm e}))^{2/3})^2 + 4\pi\rho_{\rm e}(r_{\rm e})}\}, \tag{2}$$

where $\rho_{\rm e}(r_{\rm e})$ is the electron density in the core, and $C_{\rm TF} = 3(3\pi)^{2/3}/10$ is a coefficient obtained by the Thomas-Fermi model. This exchange potential may have a slight $l_{\rm e}$ dependency [74] because the electron density depends on $l_{\rm e}$. We thus introduce a small correction for this $l_{\rm e}$ dependence. Because the squared angular momentum $l_{\rm e}(l_{\rm e}+1)$ is a good quantum number for the electron orbitals, we can modify the exchange potential as follows:

$$V_{\rm exch}^{(l_{\rm e})}(r_{\rm e}) = \left[1 - a_{\rm exch}\mathbf{l}_{\rm e}^2\right]V_{\rm exch}(r_{\rm e}), \tag{3}$$

where $\mathbf{l}_{\rm e}$ is the orbital angular momentum operator. The coefficient $a_{\rm exch}$ is assumed to have a small value. Here, the $l_{\rm e}$ dependency appears exclusively for $l_{\rm e} = 0, 1, 2$ because the range of the exchange potential is short.

The polarization potential is written as

$$V_{\rm pol}(r_{\rm e}) = -\frac{\alpha_d}{2r_{\rm e}^4}[1 - f(r_{\rm e})], \tag{4}$$

where $\alpha_d = 0.192\ a_0^3$ for Li and $\alpha_d = 0.923\ a_0^3$ for Na are the dipole polarizabilities given by Gien [75], and $f(r_{\rm e})$ is a short-range cutoff function that is determined numerically and satisfies the boundary conditions of $f(r_{\rm e} \to 0) = 1$ and $f(r_{\rm e} \to \infty) = 0$. Here, $1 - f(r_{\rm e})$ is written in exponential form [76] or polynomial form [77,78]. In this study, we expand the polarization potential in terms of Gaussian basis functions:

$$V_{\rm pol}(r_{\rm e}) = \sum_{i=1}^{N} C_i r_{\rm e}^2 {\rm e}^{-b_i r_{\rm e}^2}, \tag{5}$$

where C_i and b_i are parameters to be optimized. Although Gaussian functions decrease rapidly, a linear combination of Gaussian functions with small $0.0001 < b_i < 0.1$ can sufficiently reproduce asymptotic forms up to several tens of a.u. The short-range behavior is also effectively described. Demonstrations of this potential for nonrelativistic calculations are presented in our previous study [69]. The optimized parameters for $V_{\rm pol}(r_{\rm e})$ are listed in Appendix A.

The Schrödinger equation for a valence electron in a nonrelativistic framework can be written as

$$H_{\rm A}^{\rm nr}\psi_{n_{\rm e}l_{\rm e}} = \varepsilon_{{\rm A},\,n_{\rm e}l_{\rm e}}^{\rm nr}\psi_{n_{\rm e}l_{\rm e}}, \tag{6}$$

where

$$H_{\rm A}^{\rm nr} = -\frac{1}{2}\left\{\frac{1}{r_{\rm e}}\frac{d^2}{dr_{\rm e}^2}r_{\rm e} - \frac{l_{\rm e}(l_{\rm e}+1)}{r_{\rm e}^2}\right\} + V_{\rm e}(r_{\rm e}), \tag{7}$$

where $\psi_{n_{\rm e}l_{\rm e}}$ is the wave function of the valence electron of the alkali-metal atom, $\varepsilon_{{\rm A},\,n_{\rm e}l_{\rm e}}^{\rm nr}$ is the eigenenergy of $\psi_{n_{\rm e}l_{\rm e}}$, and $n_{\rm e}$ is

TABLE I. Calculated and observed energy levels and their absolute errors for Li and Na atoms. The notation $\Delta_{n_e l_e}$ indicates the fine structure splitting of the $n_e l_e$ state. The experimental values are taken from the NIST Atomic Spectra Database [79].

System	State	Calculation	Experiment [79]	Error $\times 10^5$
	$2s$	−0.198 140	−0.198 142	0.2
	$2p$	−0.130 243	−0.130 236	0.7
	Δ_{2p}	0.000 005	0.000 002	0.3
	$3s$	−0.074 260	−0.074 182	7.8
	$3p$	−0.057 283	−0.057 235	4.8
	$3d$	−0.055 603	−0.055 606	0.3
Li	$4s$	−0.038 653	−0.038 615	3.8
	$4p$	−0.032 001	−0.031 973	2.8
	$4d$	−0.031 272	−0.031 273	0.1
	$5s$	−0.023 657	−0.023 636	2.1
	$5p$	−0.020 389	−0.020 374	1.5
	$5d$	−0.020 012	−0.020 012	0.0
	$6s$	−0.015 957	−0.015 945	1.2
	$3s$	−0.188 857	−0.188 858	0.1
	$3p$	−0.111 558	−0.111 547	1.1
	Δ_{3p}	0.000 067	0.000 078	1.1
	$3d$	−0.056 016	−0.055 936	8.0
	$4s$	−0.071 574	−0.071 578	0.4
	$4p$	−0.050 924	−0.050 934	1.0
	Δ_{4p}	0.000 022	0.000 025	0.3
	$4d$	−0.031 487	−0.031 442	4.5
Na	$5s$	−0.037 586	−0.037 584	0.2
	$5p$	−0.029 189	−0.029 194	0.5
	Δ_{5p}	0.000 010	0.000 011	0.1
	$5d$	−0.020 132	−0.020 106	2.6
	$6s$	−0.023 133	−0.023 132	0.1
	$6p$	−0.018 914	−0.018 919	0.5
	Δ_{6p}	0.000 005	0.000 006	0.1
	$6d$	−0.013 967	−0.013 952	1.5
	$7s$	−0.015 660	−0.015 662	0.2

the principal quantum number ($n_e \geqslant 2$ for Li, and $n_e \geqslant 3$ for Na). The relativistic atomic energies $\varepsilon^{\rm rel}_{{\rm A},\,n_e l_e}$ can be written as

$$\varepsilon^{\rm rel}_{{\rm A},\,n_e l_e} = \varepsilon^{\rm nr}_{{\rm A},\,n_e l_e} + \alpha^2 \langle \psi_{n_e l_e} | H^{\rm rel}_{\rm A} | \psi_{n_e l_e} \rangle + \mathcal{O}(\alpha^3), \tag{8}$$

where the $H^{\rm rel}_{\rm A}$ is given by the Pauli approximation, namely,

$$H^{\rm rel}_{\rm A} = -\frac{1}{8}\mathbf{p}_e^4 - \frac{1}{8}\mathbf{p}_e^2 V_e + \frac{1}{2}\frac{1}{r_e}\frac{dV_e}{dr}\mathbf{l}_e \cdot \mathbf{s}_e. \tag{9}$$

$\mathbf{p}_e$ is a momentum operator. Moreover, α is the fine structure constant ($\alpha = c^{-1}$, where c is the speed of light), and $\mathbf{s}_e$ is the spin angular momentum operator for the electron.

We determine the parameters $a_{\rm exch}$ in Eq. (3) and C_i and b_i in Eq. (5) such that the calculated energy levels $\varepsilon^{\rm rel}_{{\rm A},\,nl}$ reproduce the observed energy levels and fine structure splittings [79] of the p state within an absolute error of 8×10^{-5}. The results of $a_{\rm exch}$ are 0.081 for Li and 0.00015 for Na. Table I shows that the calculated values agree well with the observed values.

According to calculations in the literature [4,6,38], the model potential between the ion core and the positron can be expressed as

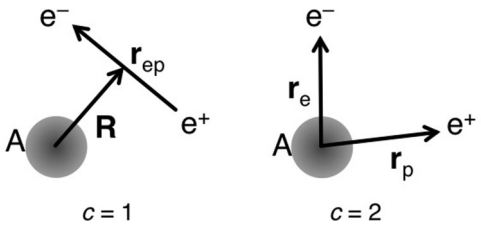

FIG. 1. Two sets of rearrangement channels and coordinates.

$$V_{\rm p}(r_{\rm p}) = -V_{\rm st}(r_{\rm p}) + V_{\rm pol}(r_{\rm p}), \tag{10}$$

where $r_{\rm p}$ is the distance between the ion core and the positron.

The nonrelativistic three-body Hamiltonian is given by

$$H^{\rm nr}_{{\rm APs}^+} = \frac{1}{2}\mathbf{p}_e^2 + \frac{1}{2}\mathbf{p}_{\rm p}^2 + V_e^{\rm nr}(r_e) + V_{\rm p}^{\rm nr}(r_{\rm p}) - \frac{1}{r_{\rm ep}} + V_{\rm 2pol}(\mathbf{r}_e, \mathbf{r}_{\rm p}) + \lambda \sum_i |\phi_i^{\rm core}\rangle\langle\phi_i^{\rm core}|, \tag{11}$$

where $V_{\rm 2pol}$ is a two-body correction to the polarization potentials for the electron and positron. Here, $V_{\rm 2pol}(\mathbf{r}_e, \mathbf{r}_{\rm p})$ was derived by Norcross and Seaton [80] and can be written as

$$V_{\rm 2pol}(\mathbf{r}_e, \mathbf{r}_{\rm p}) = 2\,\hat{\mathbf{r}}_e \cdot \hat{\mathbf{r}}_{\rm p}\sqrt{V_{\rm pol}(r_e)V_{\rm pol}(r_{\rm p})}. \tag{12}$$

The last term of the Hamiltonian (11) is introduced in order to remove pseudostates, in which the electron occupies a core orbital $\phi_i^{\rm core}$, from the total wave function [81]. We use a Gaussian expansion method (GEM), which has been applied to a variety of few-body systems (see Ref. [82] and the references therein). In Fig. 1, we introduce two rearrangement channels ($c = 1, 2$) to take the interparticle correlations into account directly. The first channel ($c = 1$) is suited to describing the configuration of $A^+ - Ps$ (Ps channel). The second channel ($c = 2$) is suited to describing the configuration of $A - e^+$ (alkali-metal atom channel). The total three-body wave function Ψ in the S state is described as the sum of the channel wave functions of the two rearrangement channels, as follows:

$$\Psi = \Phi^1(\mathbf{r}_{\rm ep}, \mathbf{R}) + \Phi^2(\mathbf{r}_e, \mathbf{r}_{\rm p}). \tag{13}$$

Each channel wave function is expanded in terms of Gaussian basis functions:

$$\Phi^c(\mathbf{x}_c, \mathbf{y}_c) = \sum_{n_c N_c l_c} A^c_{n_c N_c l_c} x_c^{l_c} y_c^{l_c} \exp\left(-\mu_{n_c} x_c^2 - \nu_{N_c} y_c^2\right) {\rm P}_{l_c}(\hat{\mathbf{x}}_c \cdot \hat{\mathbf{y}}_c), \tag{14}$$

where $(\mathbf{x}_1, \mathbf{y}_1) = (\mathbf{r}_{\rm ep}, \mathbf{R})$ and $(\mathbf{x}_2, \mathbf{y}_2) = (\mathbf{r}_e, \mathbf{r}_{\rm p})$, as shown in Fig. 1. The Gaussian range parameters μ_{n_c} and ν_{N_c} are based on a geometrical progression in order to describe both the short-range correlation and long-range tail behavior effectively. The inner angular momentum l_c can be restricted to $0 \leqslant l_c \leqslant 5$ in order to confirm the relativistic corrections in the next calculation. Here, ${\rm P}_{l_c}(\hat{\mathbf{x}}_c \cdot \hat{\mathbf{y}}_c)$ is the Legendre polynomial. The nonrelativistic three-body energy $E^{\rm nr}_{{\rm APs}^+}$ and coefficients $A^c_{n_c N_c l_c}$ in Eq. (14) are determined by the Rayleigh-Ritz variational principle.

The perturbation Hamiltonian for relativistic corrections is based on the Breit-Pauli interactions [83,84] and is written as

$$H^{\rm rel}_{\rm APs^+} = H'_{\rm mv} + H'_d + H'_{\rm oo} + H'_{\rm ss} + H'_{\rm a} + H'_{\rm so}, \tag{15}$$

where

$$H'_{\rm mv} = -\frac{1}{8}\left(\mathbf{p}_{\rm e}^4 + \mathbf{p}_{\rm p}^4\right) \tag{16}$$

$$H'_d = -\frac{1}{8}\left\{\mathbf{p}_{\rm e}^2 V_{\rm e}(r_{\rm e}) + \mathbf{p}_{\rm p}^2 V_{\rm p}(r_{\rm p})\right\} + \pi\delta(\mathbf{r}_{\rm ep}), \tag{17}$$

$$H'_{\rm oo} = \frac{1}{2}\left[\frac{\mathbf{p}_{\rm e}\cdot\mathbf{p}_{\rm p}}{r_{\rm ep}} + \frac{\mathbf{r}_{\rm ep}\cdot(\mathbf{r}_{\rm ep}\cdot\mathbf{p}_{\rm e})\mathbf{p}_{\rm p}}{r_{\rm ep}^3}\right], \tag{18}$$

$$H'_{\rm ss} = \frac{8\pi}{3}\mathbf{S}_{\rm e}\cdot\mathbf{S}_{\rm p}\delta(\mathbf{r}_{\rm ep}), \tag{19}$$

$$H'_{\rm a} = 2\pi\left(\frac{3}{4} + \mathbf{S}_{\rm e}\cdot\mathbf{S}_{\rm p}\right)\delta(\mathbf{r}_{\rm ep}), \tag{20}$$

$$\begin{aligned} H'_{\rm so} = &-\frac{(1-2\mu)}{2}\frac{\mathbf{l}_{\rm e}\cdot\mathbf{S}_{\rm e}}{r_{\rm e}}\frac{dV_{\rm e}}{dr_{\rm e}} - \frac{(1-4\mu)}{2}\frac{\mathbf{l}_{\rm ep}\cdot\mathbf{S}_{\rm p}}{r_{\rm ep}^3} \\ &+\frac{1}{4}\frac{(\mathbf{r}_{\rm ep}\times\mathbf{P})\cdot\mathbf{S}_{\rm p}}{r_{\rm ep}^3} - \frac{(1-4\mu)}{2}\frac{\mathbf{l}_{\rm ep}\cdot\mathbf{S}_{\rm e}}{r_{\rm ep}^3} \\ &-\frac{1}{4}\frac{(\mathbf{r}_{\rm ep}\times\mathbf{P})\cdot\mathbf{S}_{\rm e}}{r_{\rm ep}^3} + \frac{(1-2\mu)}{2}\frac{\mathbf{l}_{\rm p}\cdot\mathbf{S}_{\rm p}}{r_{\rm p}}\frac{dV_{\rm p}}{dr_{\rm p}}. \end{aligned} \tag{21}$$

$\mathbf{p}_{\rm e}$, $\mathbf{p}_{\rm p}$, $\mathbf{p}_{\rm ep}$, and $\mathbf{P}$ are momentum operators associated with $\mathbf{r}_{\rm e}$, $\mathbf{r}_{\rm p}$, $\mathbf{r}_{\rm ep}$, and $\mathbf{R}$, respectively, in Fig. 1. $\mathbf{S}_{\rm e}$ and $\mathbf{S}_{\rm p}$ are spin operators for the electron and positron, respectively. $\mathbf{l}_{\rm ep} = \mathbf{r}_{\rm ep}\times\mathbf{p}_{\rm ep}$ is an angular momentum operator for coordinates $\mathbf{r}_{\rm ep}$, and μ is a magnetic moment of the electron or positron. Further, $H'_{\rm mv}$ is a relativistic momentum correction, H'_d is the Darwin term, $H'_{\rm oo}$ is the retardation term, $H'_{\rm ss}$ is the spin-spin interaction, $H'_{\rm a}$ is the annihilation channel, and $H'_{\rm so}$ is the spin-orbit interaction. The relativistic correction regarding the nucleus spin can be ignored because the magnetic moment of the nucleus is three orders of magnitude smaller than that of the electron. It is noted that the spin-orbit interaction $H'_{\rm so}$ does not contribute to the relativistic correction of the current loosely bound states because the expectation values of $H'_{\rm so}$ with states of $J = 0$ vanish due to angular momentum algebra.

The total relativistic correction $\Delta\varepsilon^{\rm rel}$ is calculated using first-order perturbation theory:

$$\Delta E^{\rm rel}_{\rm APs^+} = \alpha^2\left\langle H^{\rm rel}_{\rm APs^+}\right\rangle = \alpha^2\langle\Psi|H^{\rm rel}_{\rm APs^+}|\Psi\rangle. \tag{22}$$

III. RESULTS AND DISCUSSION

We optimized the Gaussian range parameters and carefully examined the convergence of the nonrelativistic energies $E^{\rm nr}_{\rm APs^+}$ with respect to the number of Gaussian basis functions. Figure 2 shows the convergence of the nonrelativistic binding energies with respect to the number of basis functions, where one can see that $E^{\rm nr}_{\rm APs^+}$ changes slowly for $N > 4000$. We obtained converged values down to 10^{-7} a.u. accuracy in the three-body calculation, namely, for $LiPs^+$, $E^{\rm nr}_{\rm LiPs^+} = -0.252\,505\,13$ at $N = 7388$ and $E^{\rm nr}_{\rm LiPs^+} = -0.252\,505\,20$ at $N = 8404$, and for $NaPs^+$, $E^{\rm nr}_{\rm NaPs^+} = -0.250\,473\,62$ at $N = 6258$ and $E^{\rm nr}_{\rm NaPs^+} = -0.250\,473\,66$ at $N = 7266$. The nonrelativistic binding energy $\varepsilon^{\rm nr}$ associated with the dissociation threshold of $A^+ + Ps$ is given by

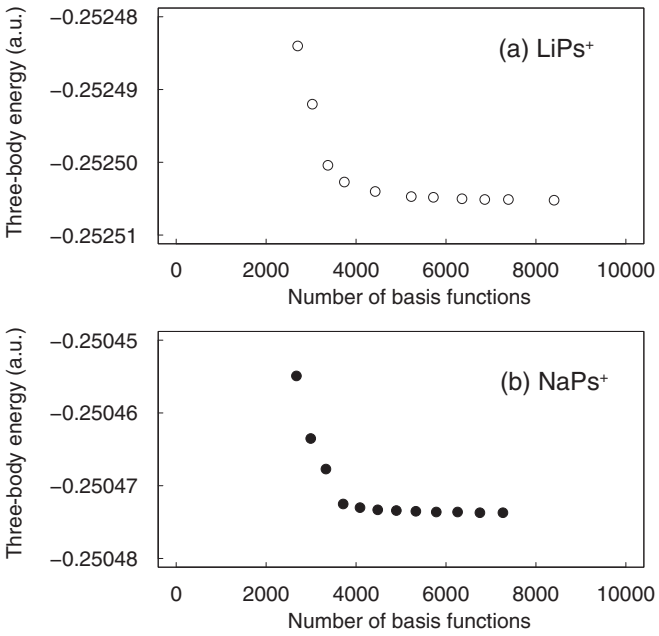

FIG. 2. Convergence of the nonrelativistic three-body energies of bound states as a function of the number of basis functions for $LiPs^+$ and $NaPs^+$. The converged values are (a) $E^{\rm nr}_{\rm LiPs^+} = -0.252\,505\,2$ and (b) $E^{\rm nr}_{\rm NaPs^+} = -0.250\,473\,7$.

$$-\varepsilon^{\rm nr} = E^{\rm nr}_{\rm APs^+} - E^{\rm nr}_{\rm Ps}, \tag{23}$$

where $E^{\rm nr}_{\rm Ps} = -0.25$.

An uncertainty of the non-relativistic binding energy, $E^{\rm nr}_{\rm APs^+}$, comes from (i) the model potential and (ii) numerical calculation. The model potential we used in this work reproduces the observed energy levels of the alkali-metal atoms at 0.2×10^{-5} a.u. for Li ($2s$) and 0.1×10^{-5} a.u. for Na ($3s$), see Table I. Since the major binding mechanism for APs^+ is Ps polarization by A^+, the uncertainty coming from the reproducibility of the model potential was estimated to be much less than 10^{-6} a.u., which was equal to the accuracy of the nonrelativistic binding energy converged. Thus, in this work, the uncertainty from (i) is not included explicitly. To determine the nonrelativistic binding energy, we solved a generalized eigenvalue problem numerically under the double precision arithmetic. We estimated and confirmed the uncertainty of numerical calculation of the nonrelativistic energy for the three-body system to be less than 10^{-9} a.u. by using different numerical methods for the eigenvalue problem.

The relativistic binding energy $\varepsilon^{\rm rel}$ is associated with the lowest dissociation threshold of $A^+ + Ps$ and is defined as follows:

$$-\varepsilon^{\rm rel} = \left(E^{\rm nr}_{\rm APs^+} + \Delta E^{\rm rel}_{\rm APs^+}\right) - \left(E^{\rm nr}_{\rm Ps} + \Delta E^{\rm rel}_{\rm Ps}\right), \tag{24}$$

where

$$\Delta E^{\rm rel}_{\rm Ps} = \alpha^2\langle\phi_{\rm Ps}|H^{\rm rel}_{\rm Ps}|\phi_{\rm Ps}\rangle. \tag{25}$$

Here, $\phi_{\rm Ps}$ is the exact Ps ($1s$) wave function and $H^{\rm rel}_{\rm Ps}$ is the perturbation Hamiltonian for relativistic corrections for Ps.

Uncertainties of the relativistic corrections $\Delta E^{\rm rel}_{\rm APs^+}$, come from (I) numerical accuracy of relativistic corrections, and

TABLE II. Binding energies of the bound state of $LiPs^+$ and $NaPs^+$ calculated in this work and previous studies.

System	Method	Binding energy
$LiPs^+$	This work (spin averaged)	0.002 509 5 (2)
	FCSVM [2,42]	0.002 478 9
	SVM [42]	0.002 482 1
	FEM [43]	0.002 37
	AHM [44]	0.002 455
	GEM [6]	0.002 615
$NaPs^+$	This work (spin averaged)	0.000 490 12 (3)
	FCSVM [40]	0.000 473
	AHM [44]	0.000 447
	GEM [6]	0.000 401
	FEM-ITM [45]	0.000 357

(II) contribution from the second-order perturbation of the relativistic corrections. As the nonrelativistic wave function is less accurate than the non-relativistic energy because of the variational principle, the calculated values of the relativistic corrections somewhat scatter even with the wave functions that give the same eigenvalue. We adopted the average and standard deviation of values calculated with different basis sets as relativistic correction and its uncertainty, respectively. Eight kinds of basis sets in total with $N = 4920$ and $N = 5778$ are used for $LiPs^+$ and four kinds of basis sets in total with $N = 4464$, 4882, 5228, and $N = 5320$ are used for $NaPs^+$. The largest uncertainty of the relativistic corrections comes from the momentum correction term, $\alpha^2\langle H'_{\rm mv}\rangle$, which is 2×10^{-7} for $LiPs^+$ and 3×10^{-8} a.u. for $NaPs^+$. On the other hand, the contribution of the second-order perturbation of the relativistic corrections (II) should be negligible for the entire uncertainty because the second-order perturbation may be lower than the first-order one by $\alpha^2 \sim 5 \times 10^{-5}$. To the end, the numerical accuracy of the relativistic corrections (I) is expected to mostly contribute to the entire uncertainty of the relativistic energy.

Table II shows the spin-averaged relativistic binding energy together with some previous results, which can be regarded as semirelativistic binding energies insofar as the model potential was constructed to reproduce the observed energy levels in a nonrelativistic framework. For $LiPs^+$, these results lie within the range of the previous results, and for $NaPs^+$, these results are slightly higher than the previous results. The differences in the results can be explained by the improvement in the polarization and exchange potentials and relativistic corrections.

In Table III, the mean radii and relativistic corrections calculated from the nonrelativistic wave function are shown for the positronic alkali-metal atoms, the corresponding alkali-metal atoms, and Ps. The spin-spin interaction $\alpha^2\langle H'_{\rm ss}\rangle$ and annihilation term $\alpha^2\langle H'_{\rm a}\rangle$ are proportional to the expectation values of the δ function $\delta(r_{\rm ep})$ according to Eqs. (19) and (20). The 2γ annihilation rate $\Gamma_{2\gamma}$ is also given in Table III. The mean radii and 2γ annihilation rates are consistent with those obtained in previous studies—for example, in [41], $\langle r_{\rm e}\rangle = 9.108\ a_0$, $\langle r_{\rm p}\rangle = 9.966\ a_0$, $\langle r_{\rm ep}\rangle = 3.397\ a_0$, and $\Gamma_{2\gamma} = 1.749 \times 10^9\ {\rm s}^{-1}$ for $LiPs^+$, and $\langle r_{\rm e}\rangle = 16.82\ a_0$, $\langle r_{\rm p}\rangle = 17.25\ a_0$, $\langle r_{\rm ep}\rangle = 3.162\ a_0$, and $\Gamma_{2\gamma} = 1.896 \times 10^9\ {\rm s}^{-1}$ for $NaPs^+$.

As shown in Table III, because of the polarization of Ps, the expectation values of the retardation term $\alpha^2\langle H'_{\rm oo}\rangle$ and the δ function $\langle\delta(r_{\rm ep})\rangle$ in APs^+ become smaller than those in isolated Ps ($1s$). On the other hand, the absolute value of the momentum correction $\alpha^2\langle H'_{\rm mv}\rangle$ and the Darwin term $\alpha^2\langle H'_d\rangle$ become much larger than those in isolated Ps ($1s$) because the relativistic electron motion in the high electric field near the nucleus also contributes to these terms.

Table IV shows the nonrelativistic and relativistic binding energies for $LiPs^+$ and $NaPs^+$ together with for related systems, namely, Li, Li^-, Na, and Na^-. The ratios of relativistic effects to the binding energy,

$$\frac{\delta\varepsilon}{\varepsilon} = \frac{\varepsilon^{\rm rel} - \varepsilon^{\rm nr}}{\varepsilon^{\rm rel}}, \tag{26}$$

are much larger than those for the host alkali-metal atoms and their negative ions. The ratios for $LiPs^+$ are 8.1 (singlet) and 31 (triplet) times larger than those for the Li atom, and those for $NaPs^+$ are 20 (singlet) and 22 (triplet) times larger than those for the Na atom.

In Fig. 3, we summarize the relativistic effect $\delta\varepsilon/\varepsilon$ for positronic atoms together with various electronic systems against the nuclear charge Z. Binding energies and relativistic corrections for Li, Na, Li^-, Na^-, $LiPs^+$, and $NaPs^+$ are given by our calculations. For hydrogenlike atoms, namely H, He^+, Li^{2+}, Na^{10+}, K^{18+}, Rb^{26+}, and Cs^{54+}, binding energies and relativistic corrections are calculated analytically for $1s$ state including momentum correction term and Darwin term in the first-order perturbation theory. For alkali-metal atoms with high $Z > 11$, namely K, Rb, Cs, and Fr, the relativistic corrections are estimated by the difference between the

TABLE III. Mean distances, relativistic corrections and 2γ annihilation rate. $\Gamma_{2\gamma}$ is given in units of $10^9\ {\rm s}^{-1}$.

	$LiPs^+$	Li ($3s$)	$NaPs^+$	Na ($3s$)	Ps ($1s$)
$\langle r_{\rm e}\rangle$	9.041 (3)	3.833	16.18 (1)	4.085	–
$\langle r_{\rm p}\rangle$	9.900 (3)	–	16.83 (3)	–	–
$\langle r_{\rm ep}\rangle$	3.399 (5)	–	3.164 (1)	–	3.000
$\alpha^2\langle H'_{\rm mv}\rangle$	−0.000 013 3 (2)	−0.000 066 3	−0.000 046 08 (3)	−0.000 920 6	−0.000 004 2
$\alpha^2\langle H'_d\rangle$	0.000 011 703(4)	0.000 052 5	0.000 032 202 (1)	0.000 639 4	0.000 006 7
$\alpha^2\langle H'_{\rm oo}\rangle$	−0.000 005 722(5)	–	−0.000 006 262 (6)	–	−0.000 006 7
$\langle\delta(r_{\rm ep})\rangle$	0.034 728 7(9)	–	0.037 760 6(1)	–	0.039 789
$\Gamma_{2\gamma}$	1.752 75(4)	–	1.905 77(1)	–	1.996

TABLE IV. Relativistic binding energies and effects of binding energy associated with dissociation threhsold of $A^+ + Ps$ for APs^+, $A + e^-$ for A^-, $A^+ + e^-$ for A and $e^+ + e^-$ for Ps.

	Spin state	$LiPs^+$	Li^- ($2s^2$)	Li ($2s$)	$NaPs^+$	Na^- ($3s^2$)	Na ($3s$)	Ps ($1s$)
$\varepsilon^{\rm nr}$		0.002 505 20	0.022 631	0.198 125 8	0.000 473 66	0.019 451	0.188 576 1	0.250 000 0
$\varepsilon^{\rm rel}$	singlet	0.002 506 6 (2)	0.022 638	0.198 139 5	0.000 488 96 (3)	0.019 472	0.188 877 3	0.250 017 5
	triplet	0.002 510 5 (2)	–		0.000 490 51 (3)	–		0.249 986 4
$(\varepsilon^{\rm rel} - \varepsilon^{\rm nr})/\varepsilon^{\rm rel}$ (%)	singlet	0.056 (8)	0.03	0.0069	3.129 (6)	0.11	0.159	0.0070
	triplet	0.211 (8)	–		3.435 (6)	–		−0.0054

energy calculated by nonrelativistic Hartree-Fock calculations [85,86] and relativistic Dirac-Fock calculations [87]. For the hydrogenlike atoms, the relativistic correction $\delta\varepsilon$ is in proportion to Z^4 and the binding energy ε is in proportion to Z^2. Thus the relativistic effect $\delta\varepsilon/\varepsilon$ is in proportion to Z^2 within the first-order perturbation theory. We found an empirical trend on the alkali-metal atoms where $\delta\varepsilon/\varepsilon$ is almost in proportion to Z^2. A simple model, $\delta\varepsilon/\varepsilon = fZ^m$ where f and m are fitting parameters, gives $m = 2.17$ and $f = 0.000\,63$ for neutral alkali-metal atoms. We can see that the trends of $LiPs^+$ and $NaPs^+$ are clearly different from the electronic systems. The largest value of $\delta\varepsilon/\varepsilon^{\rm rel}$ in Table IV, namely, 3.435(6)% for the $NaPs^+$ triplet state, is comparable to that for the neutral Cs atom, viz., 3.8%. For the negative ions of the host alkali-metal atoms, Li^- and Na^-, the ratio of relativistic effects to the binding energy are less dominant than those for positronic alkali-metal atoms while they are the systems having smaller binding energy than the neutral atoms Li and Na, respectively.

The importance of relativistic corrections in the binding energy of positronic alkali-metal atoms can be explained by positron screening of the valence electron charge. Because

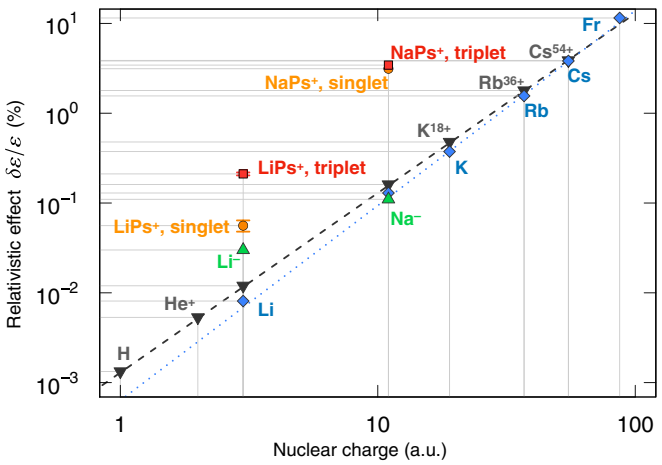

FIG. 3. Relativistic effects $\delta\varepsilon/\varepsilon$ are plotted against the nuclear charge Z for various systems. Hydrogenlike atoms (H, He^+, Li^{2+}, Na^{10+}, K^{18+}, Rb^{26+}, and Cs^{54+}) are shown in black downward triangle symbols (▽), alkali-metal atoms (Li, Na, K, Rb, Cs, and Fr) in blue diamond symbols (◇), alkali-metal negative ions (Li^- and Na^-) in green upward triangle symbols (△), positronic alkali-metal atoms ($LiPs^+$ and $NaPs^+$) in singlet states in orange circle symbols (○) and these in triplet states in red square symbols (□). The dashed line is $\delta\varepsilon/\varepsilon = fZ^m$ where $m = 2$ and $f = 0.001\,29$ and dotted line is $\delta\varepsilon/\varepsilon = fZ^m$ where $m = 2.17$ and $f = 0.000\,63$. Gray lines are guides for comparison.

Ps is neutral, the long-range interactions ($\propto r^{-1}$) between the positron or electron and the ion core are canceled out, and these results in a loosely bound state of APs^+. The distance between Ps and the ion core is two to four times larger than that for the neutral atom. The electron density, however, has a small amplitude near $r_{\rm e} = 0$ and is proportional to the valence electron density of the alkali-metal atom, whereas the positron cannot penetrate the strong Coulomb barrier of the nucleus. Thus, the valence electron is screened by the positron in the asymptotic region yet released near the nucleus, in which the relativistic effect ($\propto Z^4$) resulting from the strong attraction of the electron to the nucleus can become considerable. In ordinary atoms as well as negative ions, the nonrelativistic attraction—namely, the long-range interaction ($\propto r^{-1}$)—is dominant, and the relativistic correction in the binding energy can become less important, as shown for Li, Li^-, Na, and Na^-.

This mechanism can be supported by expectation values of fragments of the perturbation Hamiltonian. The contribution of the alkali-metal atom configuration in APs^+ to the total relativistic correction can be calculated by

$$\alpha^2\langle H^{\rm rel}_{\rm Atom}\rangle = \alpha^2\langle\Psi| - \tfrac{1}{8}\mathbf{p}_{\rm e}^4 + \tfrac{1}{8}\mathbf{p}_{\rm e}^2 V_{\rm e}(r_{\rm e})|\Psi\rangle. \quad (27)$$

The difference between the total relativistic correction and the contribution of the alkali-metal atom configuration in APs^+, $\alpha^2\langle H^{\rm rel}_{\rm APs^+}\rangle - \alpha^2\langle H^{\rm rel}_{\rm Atom}\rangle$, is roughly attributed to the relativistic correction originating from the formed Ps and A^+-e^+ repulsive correlation, whereas the correction for A^+-e^+ is much smaller than that for Ps.

Figure 4(a) illustrates nonrelativistic and relativistic level energies and relativistic corrections for $LiPs^+$. The lowest dissociation threshold $A^+ + Ps\,(1s)$ shifts to the lower side for the singlet state and to the upper side for the triplet state by a relativistic correction of $\alpha^2\langle\phi_{\rm Ps}|H^{\rm rel}_{\rm Ps}|\phi_{\rm Ps}\rangle$. The level energy of the $LiPs^+$ shifts to the lower side for the singlet state and to the upper side for the triplet state. Both of the contributions $\alpha^2\langle H^{\rm rel}_{\rm Atom}\rangle$ and $\alpha^2\langle H^{\rm rel}_{\rm APs^+}\rangle - \alpha^2\langle H^{\rm rel}_{\rm Atom}\rangle$ are negative in the singlet state. On the other hand, for the $LiPs^+$ triplet state, the contribution of the alkali-metal atom configuration $\alpha^2\langle H^{\rm rel}_{\rm Atom}\rangle$ is negative, whereas the residual contribution $\alpha^2\langle H^{\rm rel}_{\rm APs^+}\rangle - \alpha^2\langle H^{\rm rel}_{\rm Atom}\rangle$ is positive and overcomes $\alpha^2\langle H^{\rm rel}_{\rm Atom}\rangle$. The relativistic level energy of the triplet state, therefore, shifts slightly to the upper side overall.

The net relativistic correction $\delta\varepsilon$ in the binding energy is given by the difference between the relativistic corrections for the ground and dissociated states as follows:

$$\delta\varepsilon = -\varepsilon^{\rm nr} + \varepsilon^{\rm rel} = -\Delta E^{\rm rel}_{\rm APs^+} + \Delta E^{\rm rel}_{\rm Ps}. \quad (28)$$

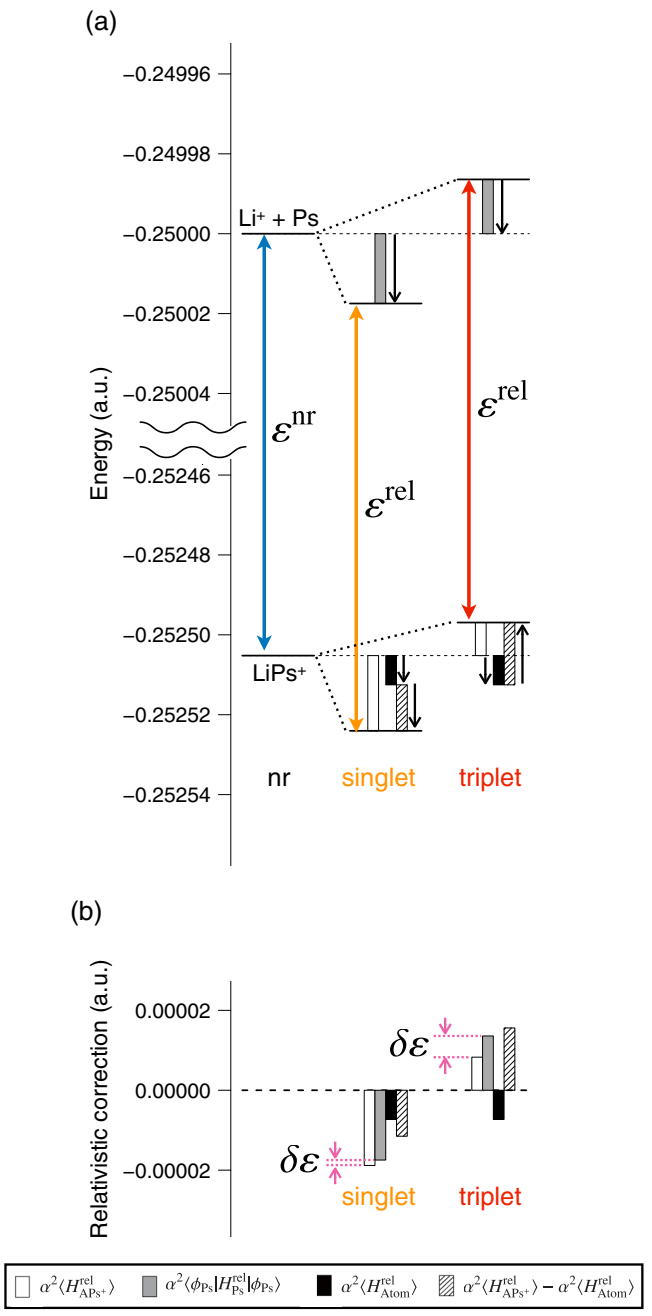

FIG. 4. (a) Energy level diagram of $LiPs^+$. Upper levels are dissociation thresholds of $Li^+ + Ps$ and lower levels are bound state of $LiPs^+$ in nonrelativistic (nr) and relativistic frameworks (spin singlet and triplet). Two-way arrows indicate the nonrelativistic and relativistic binding energies ($\varepsilon^{\rm nr}$ and $\varepsilon^{\rm rel}$). Relativistic corrections for each of the bound and dissociation states are shown in rectangles with one-way arrows. $\alpha^2\langle\phi_{\rm Ps}|H^{\rm rel}_{\rm Ps}|\phi_{\rm Ps}\rangle$ and $\alpha^2\langle H^{\rm rel}_{\rm Atom}\rangle$ are measured from the nonrelativistic level energy, and $\alpha^2\langle H^{\rm rel}_{\rm APs^+}\rangle - \alpha^2\langle H^{\rm rel}_{\rm Atom}\rangle$ is measured from the level energy shifted by $\alpha^2\langle H^{\rm rel}_{\rm Atom}\rangle$. (b) Comparison of the amount of relativistic corrections for $LiPs^+$ bound state as well as the relativistic correction of Ps. The amount of the rectangles are the same as shown in (a). The net relativistic correction $\delta\varepsilon$ corresponds to the difference between $\alpha^2\langle H^{\rm rel}_{\rm APs^+}\rangle$ and $\alpha^2\langle\phi_{\rm Ps}|H^{\rm rel}_{\rm Ps}|\phi_{\rm Ps}\rangle$.

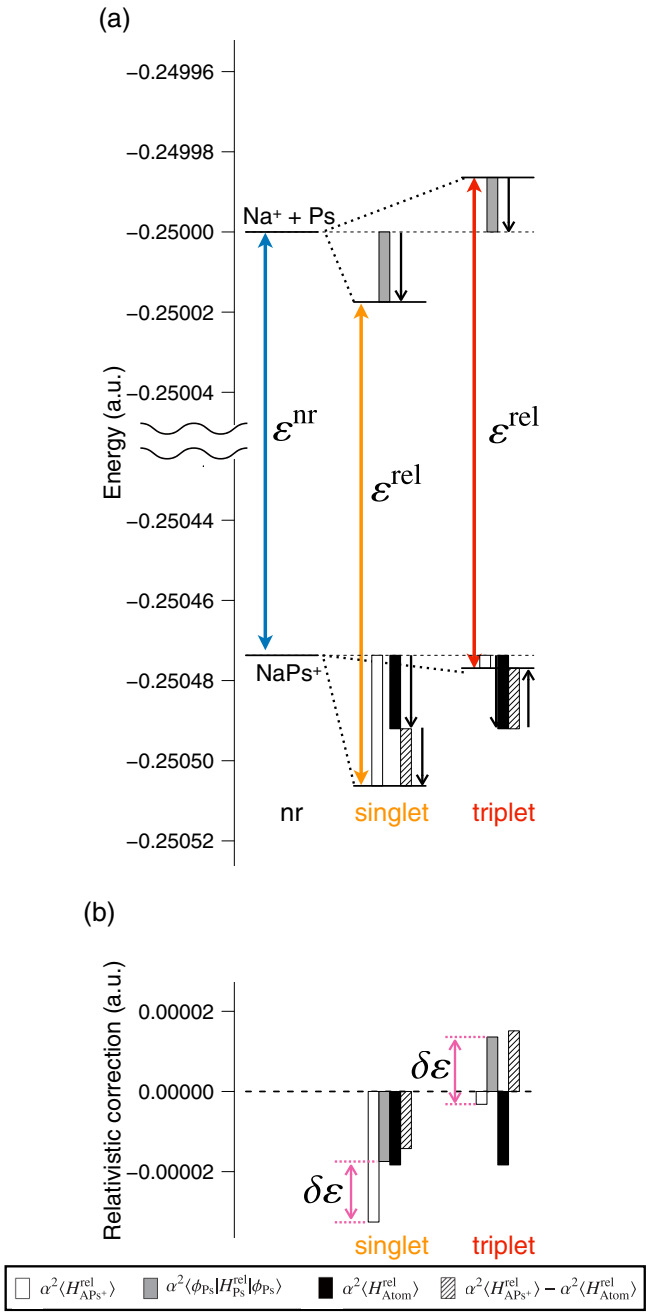

FIG. 5. (a) Energy level diagram of $NaPs^+$. Upper levels are dissociation thresholds of $Na^+ + Ps$ and lower levels are bound state of $NaPs^+$ in nonrelativistic (nr) and relativistic frameworks (spin singlet and triplet). Two-way arrows and color notation of rectangles are the same as Fig. 4(a). (b) Comparison of the amount of relativistic corrections for $NaPs^+$ bound state. The amount of the rectangles are the same as shown in Fig. 4(b).

Figure 4(b) shows the relativistic corrections for $LiPs^+$, $\Delta E^{\rm rel}_{\rm Ps} = \alpha^2\langle\phi_{\rm Ps}|H^{\rm rel}_{\rm Ps}|\phi_{\rm Ps}\rangle$, $\alpha^2\langle H^{\rm rel}_{\rm Atom}\rangle$, $\alpha^2\langle H^{\rm rel}_{\rm APs^+}\rangle - \alpha^2\langle H^{\rm rel}_{\rm Atom}\rangle$, and the total relativistic correction $\alpha^2\langle H^{\rm rel}_{\rm APs^+}\rangle$. One can see that the relativistic correction $\alpha^2\langle H^{\rm rel}_{\rm APs^+}\rangle - \alpha^2\langle H^{\rm rel}_{\rm Atom}\rangle$ has nearly the same value as the $\Delta E^{\rm rel}_{\rm Ps}$. Because the Ps in

$LiPs^+$ is only slightly deformed by the charge of the ion core, almost the entirety of the relativistic correction of e^-–e^+ in APs^+ is canceled by ΔE_{Ps}^{rel} in Eq. (28). The net relativistic correction $\delta\varepsilon$, therefore, can be attributed to the predominant contribution of the alkali-metal atom configuration $\alpha^2\langle H_{Atom}^{rel}\rangle$.

Figure 5(a) illustrates nonrelativistic and relativistic level energies and relativistic corrections for $NaPs^+$. In the $NaPs^+$ singlet state, as with the $LiPs^+$ singlet state, both of the contributions $\alpha^2\langle H_{Atom}^{rel}\rangle$ and $\alpha^2\langle H_{APs^+}^{rel}\rangle - \alpha^2\langle H_{Atom}^{rel}\rangle$ are negative. In the $NaPs^+$ triplet state, on the other hand, the negative contribution of the alkali-metal atom configuration $\alpha^2\langle H_{Atom}^{rel}\rangle$ overcomes the residual positive contribution $\alpha^2\langle H_{APs^+}^{rel}\rangle - \alpha^2\langle H_{Atom}^{rel}\rangle$. The relativistic level energy, therefore, shifts slightly to the lower side overall.

Figure 5(b) shows the relativistic corrections for $NaPs^+$. As in the case of $LiPs^+$, the relativistic correction $\alpha^2\langle H_{APs^+}^{rel}\rangle - \alpha^2\langle H_{Atom}^{rel}\rangle$ has the same value as ΔE_{Ps}^{rel}. Therefore, because of the same reason as $LiPs^+$, the net relativistic correction $\delta\varepsilon$ can be attributed to the predominant contribution of the alkali-metal atom configuration $\alpha^2\langle H_{Atom}^{rel}\rangle$.

We conclude that relativistic corrections between the ion core and valence electron are significant in a loosely bound state of APs^+, in particular contributed by e^-–A^+ interaction. It is noted that in triplet state relativistic corrections of ΔE_{Ps}^{rel} and $\alpha^2\langle H_{APs^+}^{rel}\rangle - \alpha^2\langle H_{Atom}^{rel}\rangle$ are opposite sign to $\alpha^2\langle H_{Atom}^{rel}\rangle$ while in singlet state the same sign. Thus the ratio $\delta\varepsilon/\varepsilon$ in triplet state becomes larger than that in singlet state.

IV. CONCLUSION

We investigated the binding energy of positronic alkali-metal atoms based on a three-body model in a relativistic perturbation framework. We constructed a model potential for a valence electron in an alkali-metal atom to reproduce the energy levels of an alkali-metal atom up to fine structure splittings. The binding energies of $LiPs^+$ and $NaPs^+$ were calculated based on Breit-Pauli interactions. We found that the relativistic effects are significant for the shallow binding energy of APs^+. There are two major reasons for this: (i) When the valence electron is in the asymptotic region, its charge is screened by the positron. The long-range nonrelativistic potentials cancel out each other, resulting in small binding energy. (ii) When the valence electron is near the nucleus, the electron is released from the positron and subject to significant relativistic effects. Due to the strong cancellation of the nonrelativistic energy fractions between the bound state and dissociation state, the role of the relativistic effects in the binding energy, $\delta\varepsilon/\varepsilon$, was found to be enhanced compared to that in neutral alkali-metal atoms and even their negative ions. It should be stressed that the role of the relativistic effects in $NaPs^+$ could be comparable to that in the ionization energy of the Cs atom. In other words, determining the binding energy of APs^+ with a light element A is sensitive to the relativistic effects arising from the electron motion near the nucleus. One of the advantages to consider the relativistic effects in light element systems is its validity of the first-order perturbation approximation. For example, the relativistic corrections to the binding energy of Cs^{54+} might not be converged yet up to the first-order perturbation theory.

This work casts a question on the possibility of binding of positronic potassium atom, KPs^+. The K atom has smaller ionization energy than Na atom, which implies that more Ps fraction would appear if KPs^+ had a bound state. So far, it has been shown by a model potential calculation that KPs^+ has no bound state [12]. The role enhancement of the relativistic effects in $LiPs^+$ and $NaPs^+$ found in this work could open room for re-examination of KPs^+ due to the larger nuclear charge of the K atom. Note that standard perturbation theory may not be adequate if the nonrelativistic framework could not support such a bound state. In that case a careful discussion would be required.

Our results imply that positronic atoms or molecules with a dominant Ps component may be suitable systems for investigating relativistic effects and perhaps even QED effects. Whereas the QED effects are also enhanced in heavy atoms, the perturbation expansion of the QED correction converges very slowly depending on the nuclear charge [88]. The positronic atoms of light elements have a rather simple electronic structure that be calculated with high precision, whereas heavy atoms have a number of electrons that can lead to considerable ambiguity in the theoretical calculations. Besides, the precise test of QED in atomic systems usually couples with a problem caused by the nuclear structure. The nuclear structure of the light element atoms has been rather well known. Thus, positronic systems with light elements and with the dominant Ps component could be suitable systems for investigating both relativistic and QED effects.

A precise measurement of the positronic atoms, therefore, is of importance. In addition to previously proposed methods to detect positronic atoms via charge exchange reaction [27], resonant annihilation [28], and laser-assisted photoassociation [29], recent experimental development of Ps beams [89–96] may provide a chance to measure the binding energy of the positronic atoms. Reaction from excited Ps was also proposed [30]. For example, a reaction $A + Ps \rightarrow APs^+ + e^-$ would be a subject of measurement where the emitted electron could be a monoenergetic signal. Close to the APs^+ formation threshold, there are a three-body break-up thresholds of $A + e^+ + e^-$ and/or $A^+ + e^- + e^+$; however, the energy spectrum of these three-body breakup may be distinguished from two-body rearrangement reaction, $A + Ps \rightarrow APs^+ + e^-$.

ACKNOWLEDGMENTS

T.Y. would like to thank Special Postdoctoral Researcher (SPDR) program in RIKEN, JSPS KAKENHI Grant No. JP16J02658, and financial support by the Division for Interdisciplinary Advanced Research and Education (DIARE), Tohoku University. Y.K. would like to thank JSPS KAKENHI Grants No. 17K05592 and MEXT KAKENHI No. 18H05461. The computation was carried out on the supercomputers at Kyushu University.

APPENDIX A: MATRIX ELEMENT OF SPIN-ORBIT INTERACTION OPERATOR

Optimized parameters for the polarization potentials (5) of Li and Na are listed in Tables V and VI, respectively.

TABLE V. Optimized parameters for the polarization potentials (5) of Li. Here, $x\,[y]$ denotes $x \times 10^{y}$.

i	b_i	C_i
1	2.348 260 858 827 47 [2]	−1.615 630 842 936 47 [−5]
2	8.260 865 772 027 04 [1]	−1.058 706 401 493 72 [−5]
3	4.105 150 560 834 80 [1]	−1.557 545 329 691 19 [−3]
4	1.987 700 275 134 19 [1]	−3.259 810 539 689 54 [−4]
5	1.195 656 152 364 13 [1]	−3.393 568 251 031 92 [−10]
6	8.106 999 816 821 77 [0]	−4.671 348 664 386 65 [−3]
7	6.946 156 810 093 45 [0]	−1.442 211 304 465 44 [1]
8	3.250 657 257 461 99 [0]	−4.033 864 484 436 69 [−1]
9	1.324 485 804 452 24 [0]	−1.775 039 016 749 63 [−5]
10	5.657 199 530 148 65 [−1]	−6.646 631 168 756 64 [−4]
11	1.243 790 923 296 86 [0]	−9.989 988 668 301 03 [−3]
12	1.337 105 578 580 36 [0]	−1.736 208 420 617 98 [−9]
13	7.614 409 763 004 15 [−1]	−7.431 847 225 585 93 [−7]
14	6.336 285 280 845 93 [−1]	−1.282 796 753 488 08 [−4]
15	3.715 748 452 086 13 [−1]	−3.032 785 375 196 80 [−4]
16	2.408 417 752 218 74 [−1]	−1.993 953 155 466 89 [−5]
17	1.223 451 658 524 78 [0]	−1.244 822 276 836 18 [−2]
18	5.427 494 812 023 36 [−1]	−1.117 179 578 161 56 [−3]
19	2.078 433 736 821 83 [−1]	−8.375 080 887 479 97 [−5]
20	2.239 408 777 302 18 [−1]	−1.574 188 130 032 42 [−4]
21	1.090 980 934 392 79 [−1]	−1.947 147 565 378 42 [−5]
22	1.335 879 104 085 57 [−1]	−3.848 098 040 990 84 [−5]
23	1.072 544 507 037 39 [−1]	−5.078 167 797 042 44 [−6]
24	5.574 133 245 765 09 [−2]	−6.284 395 752 377 76 [−6]
25	6.249 228 288 115 76 [−1]	−8.747 085 148 481 34 [−7]
26	2.607 462 860 414 24 [−2]	−3.226 561 230 876 73 [−7]
27	2.719 951 504 774 25 [−2]	−3.203 692 914 856 89 [−7]
28	1.485 854 882 537 86 [−2]	−3.603 057 757 850 35 [−8]
29	1.171 790 427 912 33 [−2]	−3.626 779 492 546 43 [−8]
30	1.479 529 956 194 15 [−2]	−7.839 726 549 503 17 [−9]
31	5.444 141 832 024 57 [−3]	−5.610 883 571 889 69 [−9]
32	8.138 066 070 916 65 [−3]	−9.560 946 068 594 06 [−10]
33	8.867 673 947 803 47 [−3]	−3.161 985 118 539 55 [−9]
34	2.760 859 161 913 71 [−3]	−3.942 904 979 995 06 [−10]
35	2.655 872 998 574 79 [−3]	−2.061 233 518 034 44 [−10]
36	1.497 573 638 024 65 [−3]	−7.069 367 822 069 22 [−11]
37	1.498 388 530 344 32 [−3]	−2.122 482 850 614 02 [−11]
38	1.240 554 412 628 71 [−3]	−1.266 270 285 170 48 [−11]
39	8.237 438 852 272 26 [−4]	−1.079 738 363 094 42 [−11]
40	3.480 978 659 251 25 [−4]	−3.204 139 991 288 66 [−12]

TABLE VI. Optimized parameters for the polarization potentials (5) of Na. Here, $x\,[y]$ denotes $x \times 10^{y}$.

i	b_i	C_i
1	1.895 279 736 412 12 [2]	−7.571 882 894 007 08 [−5]
2	9.801 701 309 066 59 [1]	2.310 847 720 713 46 [−5]
3	4.903 504 316 232 70 [1]	−6.915 185 870 047 49 [−4]
4	2.491 912 354 107 60 [1]	3.237 572 920 920 10 [−4]
5	1.326 906 444 857 03 [1]	−2.360 929 320 515 24 [−10]
6	7.259 433 255 168 92 [0]	−4.912 507 939 455 13 [−4]
7	3.897 758 139 597 67 [0]	−4.397 637 784 934 69 [0]
8	2.743 405 746 786 67 [0]	−8.380 900 609 964 70 [0]
9	1.023 386 060 293 19 [0]	−3.743 493 227 501 48 [−6]
10	4.310 960 468 290 70 [−1]	−1.210 021 945 950 40 [−3]
11	1.187 873 271 778 34 [0]	−2.435 186 444 327 05 [−1]
12	1.164 912 729 746 07 [0]	1.389 614 127 352 34 [−9]
13	8.866 893 564 610 15 [−1]	−1.473 385 707 231 47 [−6]
14	6.285 095 689 030 20 [−1]	−1.407 486 250 442 64 [−4]
15	7.242 332 595 306 84 [−1]	1.312 973 933 369 08 [−3]
16	3.727 063 400 793 99 [−1]	−9.114 727 029 487 20 [−6]
17	4.435 870 360 550 11 [−1]	−1.045 725 173 598 87 [−2]
18	2.052 872 492 592 96 [−1]	−3.226 441 364 256 77 [−3]
19	1.189 514 108 753 53 [−1]	−7.086 784 200 297 87 [−5]
20	1.111 178 683 596 44 [−1]	−9.375 488 342 148 87 [−5]
21	8.094 684 777 026 66 [−2]	−1.816 560 894 081 93 [−5]
22	6.694 390 239 056 50 [−2]	−2.643 328 054 515 72 [−5]
23	4.488 912 770 617 52 [−2]	−4.795 031 825 291 82 [−6]
24	3.499 333 910 599 93 [−2]	−3.699 642 607 906 34 [−6]
25	2.627 743 298 150 02 [−2]	−1.278 829 261 315 39 [−6]
26	1.804 936 967 631 64 [−2]	−3.398 210 330 440 61 [−7]
27	1.315 925 694 031 23 [−2]	−2.619 264 544 949 31 [−7]
28	9.973 452 870 100 61 [−3]	−3.515 876 322 488 74 [−8]
29	6.653 080 733 267 68 [−3]	−2.842 482 746 705 03 [−8]
30	5.441 610 354 738 76 [−3]	−6.098 964 595 869 52 [−9]
31	4.892 869 463 705 85 [−3]	−5.354 315 092 140 76 [−9]
32	3.256 113 353 648 58 [−3]	−6.980 374 591 515 64 [−10]
33	2.796 515 176 169 38 [−3]	−2.944 742 262 648 70 [−9]
34	1.656 309 307 937 64 [−3]	−3.224 586 546 424 40 [−10]
35	1.205 635 056 112 34 [−3]	−1.531 270 822 110 94 [−10]
36	1.013 294 533 403 96 [−3]	−5.982 402 799 201 86 [−11]
37	8.038 463 372 726 12 [−4]	−1.493 864 512 814 65 [−11]
38	5.475 410 390 620 09 [−4]	−8.837 316 791 774 09 [−12]
39	4.057 601 762 092 01 [−4]	−9.107 357 612 887 17 [−12]
40	2.736 472 371 157 78 [−4]	−3.231 780 450 068 60 [−12]

APPENDIX B: MATRIX ELEMENT OF SPIN-ORBIT INTERACTION OPERATOR

We here briefly show the matrix elements of the $H'_{\rm so}$ vanishes for the ground state of $LiPs^+$ and $NaPs^+$ because an orbital operator in $H'_{\rm so}$ having rank one acts on orbital angular functions of rank zero. A nonrelativistic total wave function Ψ given in different channel functions as in Eq. (13), can be rewritten in a given coordinate system $(\mathbf{x}_c, \mathbf{y}_c)$,

$$\Psi = \sum_i \mathcal{A}_i \mathcal{R}_i(x_c, y_c) \mathcal{W}_i(\hat{\mathbf{x}}_c, \hat{\mathbf{y}}_c), \tag{B1}$$

where $\mathcal{A}_i$ is a linear coefficient, $\mathcal{R}_i(x_c, y_c)$ is a radial function of x_c and y_c, $\mathcal{W}_i(\hat{\mathbf{x}}_c, \hat{\mathbf{y}}_c)$ is an spin-angular function of $\hat{\mathbf{x}}_c$ and $\hat{\mathbf{y}}_c$. $\mathcal{W}_i$ is written in the lth spherical harmonics Y_l and spin functions, χ_{s_e} and χ_{s_p} $(s_e = s_p = 1/2)$, as

$$\mathcal{W}_i(\hat{\mathbf{x}}_c, \hat{\mathbf{y}}_c) = \left[\left[Y_{l_i}(\hat{\mathbf{x}}_c) \otimes Y_{L_i}(\hat{\mathbf{y}}_c)\right]_J \otimes \left[\chi_{s_e} \otimes \chi_{s_p}\right]_S\right]_{FM} = \sum_{M_J M_S} C(JM_J SM_S|FM)\left[Y_{l_i}(\hat{\mathbf{x}}_c) \otimes Y_{L_i}(\hat{\mathbf{y}}_c)\right]_{JM_J}\left[\chi_{s_e} \otimes \chi_{s_p}\right]_{SM_S}$$

$$= \sum_{M_J M_S} \sum_{m_{l_i} m_{L_i}} \sum_{m_{s_e} m_{s_p}} C(JM_J SM_S|FM) C\left(l_i m_{l_i} L_i m_{L_i}\middle|JM_J\right) C\left(s_e m_{s_e} s_p m_{s_p}\middle|SM_S\right) Y_{l_i m_{l_i}}(\hat{\mathbf{x}}_c) \otimes Y_{L_i m_{L_i}}(\hat{\mathbf{y}}_c) \chi_{s_e m_{s_e}} \chi_{s_p m_{s_p}}, \tag{B2}$$

where J is total orbital angular momentum, S is total spin angular momentum, F is total angular momentum, and $C(j_1 m_1 j_2 m_2|jm)$ is a Clebsh-Gordan coefficient. Since the nonrelativistic Hamiltonian does not have spin-dependent term, the spin function in $\mathcal{W}_i$ can be uniquely specified. A matrix element of an operator $\hat{O}$ is given by

$$\mathcal{M}_{ij}[\hat{O}] = \mathcal{A}_i \mathcal{A}_j \langle \mathcal{R}_i \mathcal{W}_i | \hat{O} | \mathcal{R}_j \mathcal{W}_j \rangle. \tag{B3}$$

We first evaluate the angular integration of $\mathcal{M}_{ij}$. The spin–orbit term involves six different operators, namely,

$$\hat{O}_1 = \frac{\mathbf{l}_\mathrm{e} \cdot \mathbf{S}_\mathrm{e}}{r_\mathrm{e}} \frac{dV_\mathrm{e}}{dr_\mathrm{e}}, \tag{B4}$$

$$\hat{O}_2 = \frac{\mathbf{l}_\mathrm{ep} \cdot \mathbf{S}_\mathrm{p}}{r_\mathrm{ep}^3}, \tag{B5}$$

$$\hat{O}_3 = \frac{\mathbf{l}_\mathrm{ep} \cdot \mathbf{S}_\mathrm{e}}{r_\mathrm{ep}^3}, \tag{B6}$$

$$\hat{O}_4 = \frac{\mathbf{l}_\mathrm{p} \cdot \mathbf{S}_\mathrm{p}}{r_\mathrm{p}} \frac{dV_\mathrm{p}}{dr_\mathrm{p}}, \tag{B7}$$

$$\hat{O}_5 = \frac{(\mathbf{r}_\mathrm{ep} \times \mathbf{P}) \cdot \mathbf{S}_\mathrm{p}}{r_\mathrm{ep}^3}, \tag{B8}$$

and,

$$\hat{O}_6 = \frac{(\mathbf{r}_\mathrm{ep} \times \mathbf{P}) \cdot \mathbf{S}_\mathrm{e}}{r_\mathrm{ep}^3}. \tag{B9}$$

Evaluation of the matrix element $\mathcal{M}_{ij}[\hat{O}_k]$ ($k = 1$–6) can be divided into angular part and radial part. The matrix element of $\hat{O}_1$ can be written in irreducible representation [97],

$$\mathcal{M}_{ij}[\hat{O}_1] = \mathcal{A}_i \mathcal{A}_j \langle \mathcal{R}_i \mathcal{W}_i | \hat{O}_1 | \mathcal{R}_j \mathcal{W}_j \rangle = \mathcal{A}_i \mathcal{A}_j \frac{1}{\sqrt{2F+1}} \langle \mathcal{W}_i \| \mathbf{l}_\mathrm{e} \cdot \mathbf{S}_\mathrm{e} \| \mathcal{W}_j \rangle \langle \mathcal{R}_i | \frac{1}{r_\mathrm{e}} \frac{dV_\mathrm{e}}{dr_\mathrm{e}} | \mathcal{R}_j \rangle. \tag{B10}$$

The angular integration is further reduced using a relationship between scalar product $\mathbf{l}_\mathrm{e} \cdot \mathbf{S}_\mathrm{e}$ and irreducible tensor product $[\hat{l}_\mathrm{e} \otimes \hat{S}_\mathrm{e}]_0$,

$$\begin{aligned}
\langle \mathcal{W}_i \| \mathbf{l}_\mathrm{e} \cdot \mathbf{S}_\mathrm{e} \| \mathcal{W}_j \rangle &= -\sqrt{3} \langle \mathcal{W}_i \| [\hat{l}_\mathrm{e} \otimes \hat{S}_\mathrm{e}]_0 \| \mathcal{W}_j \rangle \\
&= -3(2F+1) \begin{Bmatrix} J & S & F \\ J & S & F \\ 1 & 1 & 0 \end{Bmatrix} \langle \left[Y_{l_i}(\hat{\mathbf{x}}_c) \otimes Y_{L_i}(\hat{\mathbf{y}}_c) \right]_J \| \hat{l}_\mathrm{e} \| \left[Y_{l_j}(\hat{\mathbf{x}}_c) \otimes Y_{L_j}(\hat{\mathbf{y}}_c) \right]_J \rangle \langle \left[\chi_{s_\mathrm{e}} \otimes \chi_{s_\mathrm{p}} \right]_S \| \hat{S}_\mathrm{e} \| \left[\chi_{s_\mathrm{e}} \otimes \chi_{s_\mathrm{p}} \right]_S \rangle.
\end{aligned} \tag{B11}$$

Here, $\{\cdots\}$ is the Wigner's $9j$ symbol, which vanishes unless a triangular conditions are fulfilled for triads $(J, J, 1)$, $(S, S, 1)$, $(F, F, 0)$, and (J, S, F). One can see that in $J = 0$, the Wigner's $9j$ symbol vanishes because the triad $(J, J, 1)$ cannot be fulfilled. In other words, the angular part of the nonrelativistic wave function of $LiPs^+$ and $NaPs^+$ written in rank zero ($J = 0$) vanishes in the integration with the angular operator $\mathbf{l}_\mathrm{e}$ of rank one. The matrix element $\mathcal{M}_{ij}[\hat{O}_1]$, therefore, has no contribution to $\langle H'_\mathrm{so} \rangle$. In the same reason, matrix elements $\mathcal{M}_{ij}[\hat{O}_k]$ ($k = 1$–4) have no contribution to $\langle H'_\mathrm{so} \rangle$.

The matrix element of $\hat{O}_5$ is written as,

$$\begin{aligned}
\mathcal{M}_{ij}[\hat{O}_5] &= \mathcal{A}_i \mathcal{A}_j \langle \mathcal{R}_i \mathcal{W}_i | \hat{O}_5 | \mathcal{R}_j \mathcal{W}_j \rangle \\
&= \mathcal{A}_i \mathcal{A}_j \frac{1}{\sqrt{2F+1}} \langle \mathcal{R}_i \mathcal{W}_i \| \hat{O}_5 \| \mathcal{R}_j \mathcal{W}_j \rangle \\
&= \mathcal{A}_i \mathcal{A}_j \frac{1}{\sqrt{2F+1}} \Big\{ \sqrt{6} \langle \mathcal{W}_i \| [[\hat{r}_\mathrm{ep} \otimes \hat{R}]_1 \otimes \hat{S}_\mathrm{e}]_0 \| \mathcal{W}_j \rangle \langle \mathcal{R}_i | r_\mathrm{ep} \frac{\partial}{\partial R} | \mathcal{R}_j \rangle \\
&\quad + \sqrt{12} \langle \mathcal{W}_i \| [[\hat{r}_\mathrm{ep} \otimes [\hat{R} \otimes \hat{L}]_1]_1 \otimes \hat{S}_\mathrm{e}]_0 \| \mathcal{W}_j \rangle \langle \mathcal{R}_i | \frac{r_\mathrm{ep}}{R} | \mathcal{R}_j \rangle \Big\},
\end{aligned} \tag{B12}$$

where $\hat{L}$ is angular momentum operator on coordinate $\mathbf{R}$. The angular part of the first term of Eq. (B12) can be reduced as

$$\begin{aligned}
&\langle \mathcal{W}_i \| [[\hat{r}_\mathrm{ep} \otimes \hat{R}]_1 \otimes \hat{S}_\mathrm{e}]_0 \| \mathcal{W}_j \rangle \\
&= (2F+1) \begin{Bmatrix} J & S & F \\ J & S & F \\ 1 & 1 & 0 \end{Bmatrix} \langle \left[Y_{l_i}(\hat{\mathbf{r}}_\mathrm{ep}) \otimes Y_{L_i}(\hat{\mathbf{R}}) \right]_J \| [\hat{r}_\mathrm{ep} \otimes \hat{R}]_1 \| \left[Y_{l_j}(\hat{\mathbf{r}}_\mathrm{ep}) \otimes Y_{L_j}(\hat{\mathbf{R}}) \right]_J \rangle \langle \left[\chi_{s_\mathrm{e}} \otimes \chi_{s_\mathrm{p}} \right]_S \| \hat{S}_\mathrm{e} \| \left[\chi_{s_\mathrm{e}} \otimes \chi_{s_\mathrm{p}} \right]_S \rangle.
\end{aligned} \tag{B13}$$

The angular part in the latter term is reduced as

$$\langle \mathcal{W}_i \| [[\hat{r}_{\rm ep} \otimes [\hat{R} \otimes \hat{L}_c]_1]_1 \otimes \hat{S}_{\rm e}]_0 \| \mathcal{W}_j \rangle = (2F+1) \begin{Bmatrix} J & S & F \\ J & S & F \\ 1 & 1 & 0 \end{Bmatrix} \langle \left[Y_{l_i}(\hat{\mathbf{r}}_{\rm ep}) \otimes Y_{L_i}(\hat{\mathbf{R}}) \right]_J \| [\hat{r}_{\rm ep} \otimes [\hat{R} \otimes \hat{L}]_1]_1 \| \left[Y_{l_j}(\hat{\mathbf{r}}_{\rm ep}) \otimes Y_{L_j}(\hat{\mathbf{R}}) \right]_J \rangle$$
$$\times \langle \left[\chi_{s_{\rm e}} \otimes \chi_{s_{\rm p}} \right]_S \| \hat{S}_{\rm e} \| \left[\chi_{s_{\rm e}} \otimes \chi_{s_{\rm p}} \right]_S \rangle. \tag{B14}$$

In the same reason as $\mathcal{M}_{ij}[\hat{O}_k]$ ($k = 1$–4), the Wigner's $9j$ symbol becomes zero in $J = 0$. Therefore, $\mathcal{M}_{ij}[\hat{O}_5]$ neither contributes to $\langle H'_{\rm so} \rangle$. Similarly, $\mathcal{M}_{ij}[\hat{O}_6]$ has no contribution to $\langle H'_{\rm so} \rangle$. Thus in total $\langle H'_{\rm so} \rangle$ has no contribution in relativistic corrections of positronic alkali-metal atoms.

[1] C. M. Surko, G. F. Gribakin, and S. J. Buckman, J. Phys. B: At. Mol. Opt. Phys. **38**, R57 (2005).
[2] J. Mitroy, Phys. Rev. Lett. **94**, 033402 (2005).
[3] V. Rotival, K. Bennaceur, and T. Duguet, Phys. Rev. C **79**, 054309 (2009).
[4] G. G. Ryzhikh and J. Mitroy, Phys. Rev. Lett. **79**, 4124 (1997).
[5] J. Mitroy, M. W. J. Bromley, and G. Ryzhikh, J. Phys. B **35**, R81 (2002).
[6] Y. Kubota and Y. Kino, New J. Phys. **10**, 023038 (2008).
[7] K. Strasburger, J. Chem. Phys. **144**, 144316 (2016).
[8] T. Yamashita, M. Umair, and Y. Kino, J. Phys. B: At. Mol. Opt. Phys. **50**, 205002 (2017).
[9] K. Strasburger and H. Chojnacki, Chem. Phys. Lett. **241**, 485 (1995).
[10] M. W. J. Bromley and J. Mitroy, Phys. Rev. A **66**, 062504 (2002).
[11] V. A. Dzuba, V. V. Flambaum, G. F. Gribakin, and W. A. King, Phys. Rev. A **52**, 4541 (1995).
[12] X. Cheng, D. Babikov, and D. M. Schrader, Phys. Rev. A **83**, 032504 (2011).
[13] X. Cheng, D. Babikov, and D. M. Schrader, Phys. Rev. A **85**, 012503 (2012).
[14] S. J. Ward, M. Horbatsch, R. P. McEachran, and A. D. Stauffer, J. Phys. B: At. Mol. Opt. Phys. **22**, 3763 (1989).
[15] F. Liu, Y. Cheng, Y. Zhou, and L. Jiao, Phys. Rev. A **83**, 032718 (2011).
[16] S. J. Ward and J. Shertzer, New J. Phys. **14**, 025003 (2012).
[17] L. Jiao, Y. Zhou, Y. Cheng, and R. Yu, Eur. Phys. J. D **66**, 48 (2012).
[18] Y. K. Ho, Phys. Rev. A **38**, 6424 (1988).
[19] A. Igarashi and I. Shimamura, Phys. Rev. A **56**, 4733 (1997).
[20] Y. K. Ho, Nucl. Instrm. Phys. Res. B **266**, 516 (2008).
[21] S. Kar and Y. K. Ho, Eur. Phys. J. D **35**, 453 (2005).
[22] J. R. Machacek, R. Boadle, S. J. Buckman, and J. P. Sullivan, Phys. Rev. A **86**, 064702 (2012).
[23] M. Umair and S. Jonsell, Phys. Rev. A **92**, 012706 (2015).
[24] M. Umair and S. Jonsell, J. Phys. B: At. Mol. Opt. Phys. **49**, 015004 (2016).
[25] T. Yamashita and Y. Kino, Eur. Phys. J. D **70**, 190 (2016).
[26] T. Yamashita and Y. Kino, Eur. Phys. J. D **72**, 13 (2018).
[27] J. Mitroy and G. G. Ryzhikh, J. Phys. B: At. Mol. Opt. Phys. **32**, L411 (1999).
[28] V. A. Dzuba, V. V. Flambaum, and G. F. Gribakin, Phys. Rev. Lett. **105**, 203401 (2010).
[29] C. M. Surko, J. R. Danielson, G. F. Gribakin, and R. E. Continetti, New J. Phys. **14**, 065004 (2012).
[30] A. R. Swann, D. B. Cassidy, A. Deller, and G. F. Gribakin, Phys. Rev. A **93**, 052712 (2016).
[31] S. Zhou, S. P. Parikh, W. E. Kauppila, C. K. Kwan, D. Lin, A. Surdutovich, and T. S. Stein, Phys. Rev. Lett. **73**, 236 (1994).
[32] G. Ryzhikh and J. Mitroy, J. Phys. B **30**, 5545 (1997).
[33] C. Campbell, M. T. McAlinden, A. A. Kernoghan, and H. Walters, Nucl. Instrum. Meth. Phys. Res. B **143**, 41 (1998).
[34] E. Surdutovich, J. M. Johnson, W. E. Kauppila, C. K. Kwan, and T. S. Stein, Phys. Rev. A **65**, 032713 (2002).
[35] A.-T. Le, M. W. J. Bromley, and C. D. Lin, Phys. Rev. A **71**, 032713 (2005).
[36] A. V. Lugovskoy, A. S. Kadyrov, I. Bray, and A. T. Stelbovics, Phys. Rev. A **85**, 034701 (2012).
[37] K. Strasburger and H. Chojnacki, J. Chem. Phys. **108**, 3218 (1998).
[38] G. Ryzhikh, J. Mitroy, and K. Varga, J. Phys. B: At. Mol. Opt. Phys. **31**, 3965 (1998).
[39] J. Yuan, B. D. Esry, T. Morishita, and C. D. Lin, Phys. Rev. A **58**, R4 (1998).
[40] J. Mitroy, M. W. J. Bromley, and G. Ryzhikh, J. Phys. B: At. Mol. Opt. Phys. **32**, 2203 (1999).
[41] J. Mitroy and G. Ryzhikh, J. Phys. B: At. Mol. Opt. Phys. **32**, L621 (1999).
[42] J. Mitroy, Phys. Rev. A **70**, 024502 (2004).
[43] J. Shertzer and S. J. Ward, Phys. Rev. A **73**, 022504 (2006).
[44] H.-l. Han, Y. Li, X.-z. Zhang, and T.-y. Shi, J. Chem. Phys. **128**, 244314 (2008).
[45] J. Shertzer and S. J. Ward, Phys. Rev. A **81**, 064505 (2010).
[46] P. Pyykkö, Chem. Rev. **88**, 563 (1988).
[47] P. Pyykkö, Ann. Rev. Phys. Chem. **63**, 45 (2012).
[48] P. Schwerdtfeger, M. Dolg, W. H. E. Schwarz, G. A. Bowmaker, and P. D. W. Boyd, J. Chem. Phys. **91**, 1762 (1989).
[49] P. Schwerdtfeger, J. Am. Chem. Soc. **111**, 7261 (1989).
[50] P. Schwerdtfeger, P. D. W. Boyd, A. K. Burrell, W. T. Robinson, and M. J. Taylor, Inorg. Chem. **29**, 3593 (1990).
[51] P. Schwerdtfeger, P. D. W. Boyd, S. Brienne, and A. K. Burrell, Inorg. Chem. **31**, 3411 (1992).
[52] P. Schwerdtfeger and G. A. Bowmaker, J. Chem. Phys. **100**, 4487 (1994).
[53] R. Wesendrup, J. K. Laerdahl, and P. Schwerdtfeger, J. Chem. Phys. **110**, 9457 (1999).
[54] A. Muñoz-Castro, J. Phys. Chem. Lett. **4**, 3363 (2013).
[55] G.-J. Cao, W. H. E. Schwarz, and J. Li, Inorg. Chem. **54**, 3695 (2015).
[56] G. Ciancaleoni, S. Rampino, D. Zuccaccia, F. Tarantelli, P. Belanzoni, and L. Belpassi, J. Chem. Theory Comput. **10**, 1021 (2014).

[57] P. Pyykkö, Chem. Rev. **112**, 371 (2012).
[58] A. Türler and V. Pershina, Chem. Rev. **113**, 1237 (2013).
[59] H.-T. Liu, D.-L. Huang, Y. Liu, L.-F. Cheung, P. D. Dau, C.-G. Ning, and L.-S. Wang, J. Phys. Chem. Lett. **6**, 637 (2015).
[60] T. Saue, Chem. Phys. Chem. **12**, 3077 (2011).
[61] M. Dolg and X. Cao, Chem. Rev. **112**, 403 (2012).
[62] H. Nakatsuji, Acc. Chem. Res. **45**, 1480 (2012).
[63] J. Seino and H. Nakai, Int. J. Quantum Chem. **115**, 253 (2015).
[64] M. S. Safronova, D. Budker, D. DeMille, D. F. J. Kimball, A. Derevianko, and C. W. Clark, Rev. Mod. Phys. **90**, 025008 (2018).
[65] S. L. Saito, Chem. Phys. Lett. **503**, 331 (2011).
[66] V. A. Dzuba, V. V. Flambaum, G. F. Gribakin, and C. Harabati, Phys. Rev. A **86**, 032503 (2012).
[67] C. Harabati, V. A. Dzuba, and V. V. Flambaum, Phys. Rev. A **89**, 022517 (2014).
[68] T. Yamashita, A. Irisawa, and Y. Kino, JJAP Conf. Proc. **2**, 011005 (2014).
[69] T. Yamashita and Y. Kino, J. Phys.: Conf. Ser. **618**, 012009 (2015).
[70] D. R. Hartree, Proc. Camb. Phil. Soc. **24**, 111 (1928).
[71] J. Mitroy, Ph.D. thesis, University of Melbourne, 1983.
[72] J. B. Furness and I. E. McCarthy, J. Phys. B **6**, 2280 (1973).
[73] F. A. Gianturco and S. Scialla, J. Phys. B **20**, 3171 (1987).
[74] K. Bartschat, *Computational Atomic Physics* (Springer, Berlin, 1996), Chap. 2, p. 15.
[75] T. Gien, Phys. Rev. A **35**, 2026 (1987).
[76] B. J. Albright, K. Bartschat, and P. R. Flicek, J. Phys. B: At. Mol. Opt. Phys. **26**, 337 (1993).
[77] G. Peach, H. E. Saraph, and M. J. Seaton, J. Phys. B: At. Mol. Opt. Phys. **21**, 3669 (1988).
[78] G. Peach, Comments At. Mol. Phys. **11**, 101 (1982).
[79] A. Kramida, Yu. Ralchenko, J. Reader, and NIST ASD Team, NIST Atomic Spectra Database (ver. 5.7), https://physics.nist.gov/asd. National Institute of Standards and Technology, Gaithersburg, 2019.
[80] D. W. Norcross and M. J. Seaton, J. Phys. B: At. Mol. Phys. **9**, 2983 (1976).
[81] V. M. Krasnopolsky and V. I. Kukulin, Sov. J. Nucl. Phys. **20**, 883 (1974).
[82] E. Hiyama, Y. Kino, and M. Kamimura, Prog. Part. Nucl. Phys. **51**, 223 (2003).
[83] H. A. Bethe and E. E. Salpeter, *Quantum Mechanics of One- and Two-Electron Atoms* (Plenum, New York, 1977).
[84] E. M. L. V. B. Berestetskii and L. P. Pitaevskii, *Kvantovaya Elektrodinamika (Quantum Electrodynamics)* (Nauka, Moscow, 1989).
[85] C. F. Bunge, J. A. Barrientos, and A. V. Bunge, At. Data Nucl. Data Tables **53**, 113 (1993).
[86] A. D. McLean and R. S. McLean, At. Data Nucl. Data Tables **26**, 197 (1981).
[87] J. P. Desclaux, At. Data Nucl. Data Tables **12**, 311 (1973).
[88] W. Kutzelnigg, Chem. Phys. **395**, 16 (2012).
[89] B. L. Brown, *Positron Annihilation*, edited by P. C. Jain, R. M. Singru, and K. P. Gopinathan (World Scientific, Singapore, 1985).
[90] G. Laricchia and H. R. J. Walters, La Rivista del Nuovo Cimento **35**, 305 (2012).
[91] K. Michishio, T. Tachibana, R. H. Suzuki, K. Wada, A. Yagishita, T. Hyodo, and Y. Nagashima, Appl. Phys. Lett. **100**, 254102 (2012).
[92] S. J. Brawley, S. E. Fayer, M. Shipman, and G. Laricchia, Phys. Rev. Lett. **115**, 223201 (2015).
[93] A. Deller, A. M. Alonso, B. S. Cooper, S. D. Hogan, and D. B. Cassidy, Phys. Rev. Lett. **117**, 073202 (2016).
[94] A. C. L. Jones, J. Moxom, H. J. Rutbeck-Goldman, K. A. Osorno, G. G. Cecchini, M. Fuentes-Garcia, R. G. Greaves, D. J. Adams, H. W. K. Tom, A. P. Mills, and M. Leventhal, Phys. Rev. Lett. **119**, 053201 (2017).
[95] A. M. Alonso, B. S. Cooper, A. Deller, L. Gurung, S. D. Hogan, and D. B. Cassidy, Phys. Rev. A **95**, 053409 (2017).
[96] K. Michishio, L. Chiari, F. Tanaka, N. Oshima, and Y. Nagashima, Rev. Sci. Instrum. **90**, 023305 (2019).
[97] D. A. Varshalovich, A. N. Moskalev, and V. K. Khersonskii, *Quantum Theory of Angular Momentum* (World Scientific, Singapore, 1988).